Microstructure and mechanical property formation of heat treated low-carbon chromium-nickel-molybdenum steels

M. V. Maisuradze · A. A. Kuklina · V. V. Nazarova · M. A. Ryzhkov · E. V. Antakov

Received: 24 August 2023 / Revised: 30 September 2023 / Accepted: 15 December 2023 / Published online: 8 July 2024

Abstract
Low-carbon Cr-Ni-Mo steels widely used in mechanical engineering are studied: 18Kh2N4MA, 25Kh2N4MA, 25KhN3MA. Thermokinetic diagrams are plotted by a dilatometric method. Temperature-time ranges for microstructure constituent formation are established. It is shown that bainite within the steels studied may be formed both above and below the M_s temperature. Features of isothermal bainite transformation are investigated, kinetics of bainite transformation are determined, as well as the quantitative ratio of microstructure constituents formed as a result of austempering. It is established that the largest amount of bainite within the steel structures studied (80–95%) is achieved at a temperature near M_s. Mechanical properties (strength, ductility, impact strength) of the steels being studied are analyzed after various heat treatment methods: various cooling intensities, upper and lower bainite austempering. It is shown that formation of upper bainite has an ambiguous effect on steel impact strength.

Keywords Steel · Heat treatment · Dilatometry · Austenite transformation · Mechanical properties · Bainite · Martensite.

Introduction

Low-carbon alloy tool steels are used extensively for preparing critical components operating under severe loading and wear conditions [1, 2]. After carburizing and hardening the surface of these components acquires high hardness and wear resistance. In this case it is important that the core of surface strengthened components exhibits simultaneously adequate strength, ductility, and impact strength for the purpose of reducing sensitivity towards crack formation during operation. A similar combination of mechanical properties is normally achieved with formation during heat treatment of a bainitic or a bainitic-martensitic structure [3–5].

A bainitic-martensitic structure within alloy steels may form both during continuous cooling (for example during normalizing or convective cooling within a gas stream), and also during isothermal quenching [6–8]. In the case of continuous cooling the steel microstructure will consists of a mixture of bainite of different morphology, formed within different temperature ranges. Isothermal quenching facilitates formation of a more uniform bainitic structure. It is well known [9, 10] that upper bainite within the majority of steels exhibits reduced strength and ductility as a result of separation of coarse carbide particles between α-phase bainite lamellae, and therefore formation of upper bainite during heat treatment is extremely undesirable. Conversely

Translated from *Metallurg*, No. 3, pp. 21–30, March, 2024. Russian DOI: https://doi.org/10.52351/00260827_2024_3_21

lower bainite more often exhibits good impact strength with retention of adequate strength, which reduces separation of fine carbide particles within platelets of martensitic type α-phase [10, 11].

In the course of bainite formation alongside carbide particle formation there is diffusion redistribution of carbon between platelets forming α-phase and the surrounding unconverted austenite [12, 13]. Depending upon steel chemical composition these processes will compete with each other. For example, in steels alloyed with silicon and aluminum the carbide formation process is difficult, and therefore untransformed austenite will be enriched to a greater extent with carbon during bainite formation [14]. A change in the chemical composition of untransformed austenite leads to a shift in the martensitic transformation temperature range into a lower temperature region, down to negative, which becomes a reason for stabilization of residual austenite within the steel structure after cooling to room temperature. Residual austenite facilitates development of a TRIP-effect during steel deformation: during load application residual austenite is converted into strain-induced martensite, as a result of which there is additional metal strengthening [15].

It has been demonstrated in a number of works [16, 17] that the best set of steel mechanical properties is achieved in the case of forming during heat treatment a mixed bainite-martensite structure. However, in some cases formation of even a small amount of bainite leads to a marked reduction in steel toughness-ductility properties [18]. The features observed are connected with the fact that within steels of different alloys systems the nature of processes occurring during bainite formation differ considerably.

Features of bainite-martensite microstructure formation over a wide and extensively used nickel-containing carburized steels used extensively in industry are studied in the present work under different heat treatment conditions with the aim of achieving the optimum ratio of a high strength level and toughness-ductility properties.

Research material and procedure

In this work industrial nickel-containing steels 18Kh2N4MA, 25Kh2N4MA, and 25KhN3MA are studied, used in engineering for heavily loaded carburized components (gear wheels, shafts, etc.). The steel chemical compositions are provided in Table 1.

A study of transformation of supercooled austenite, proceeding during continuous cooling from the austenitizing temperature and during isothermal quenching, is accomplished by means of a LINSEIS L78R.I.T.A high-speed induction dilatometer. Heating of specimens (diameter 4 mm, length 10 mm) to the austenitizing temperature (880 °C) and exposure (15 min) were conducted within a dilatometer vacuum chamber. Continuous cooling from the austenitizing temperature to room temperature was accomplished within a stream of helium at a constant rate of 0.1–30 °C/sec.

Analysis of dilatometric curves with the aim of constructing a dependence of the proportion of austenite transformation on temperature was conducted by a procedure provided in [19] in accordance with an equation

$$P = \frac{\{\Delta l_t - (a_\gamma t + b_\gamma)\}}{\{(a_\alpha t + b_\alpha) - (a_\gamma t + b_\gamma)\}}, \quad (1)$$

where P is proportion of transformed austenite; t is specimen current temperature; Δl_t is specimen current elongation at a given temperature, μm; a_γ, b_γ are linear equation coefficients approximating an experimental dilatogram within single-phase austenitic regions; a_α, b_α are linear equation coefficients approximating a speci-

Table 1 Test Steel Chemical Composition, w.t%

Steel	C	Cr	Mn	Si	Ni	Mo	S	P	Cu
18Kh2N4MA	0.19	1.44	0.40	0.34	4.05	0.31	0.005	0.007	0.10
25Kh2N4MA	0.27	1.42	0.43	0.26	4.14	0.29	0.011	0.011	0.16
25KhN3MA	0.24	1.18	0.65	0.20	2.85	0.20	0.025	0.009	0.13

men experimental dilatogram after completion of isothermal bainitic transformation. As a result the instantaneous proportion of austenite was determined at each temperature during performance of an experiment.

Plotting austenite transformation thermokinetic diagrams within test steels was accomplished in the form of recommendations [20].

Dilatometric study of the isothermal quenching process was performed with the following experimental conditions: austenitizing temperature 880 °C, exposure time 15 min, cooling at a rate of 20 °C/sec to the isothermal quenching temperature (250, 300, 330, 370, 400, 430 °C), exposure at this temperature for 3 h, and cooling to room temperature. Isothermal transformation kinetics were determined from the original dilatometric curves by the procedure in [7].

In order to study mechanical properties laboratory heat treatment was performed for specimens with dimensions of 15X15X70 mm. Heating to the austenitizing temperature of 880 °C was performed within a SNOL furnace, exposure time 60 min. Subsequent specimen cooling to room temperature was accomplished within different media: quenching oil I20A, still air, and a heat-insulated container, filled with cast iron shavings. In this case the average specimen cooling rate achieved within the temperature range of bainitic and martensitic transformation (200–500 °C) according to previous studies [21] comprises 20 °C/sec during cooling in oil, 1 °C/sec during cooling within still air, and 0.2 °C/sec during cooling within a container.

During implementation of isothermal quenching of a specimen after heating to the austenitizing temperature 880 °C it was transferred to a SShOL furnace-bath with molten slat (50% KNO_3 + 50% $NaNO_3$). The isothermal quenching temperature was selected in order that within the structure of each steel there was formation of either lower or upper bainite (for steel 18Kh2N4MA it was 330 and 400 °C for steel 25Kh2N4MA it was 280 and 370 °C, and for steel 25KhN3MA it was 280 and 400 °C). The exposure time at the isothermal quenching temperature was 2 h. Cooling after isothermal exposure was performed in quenching oil I20A. After strengthening heat treatment (cooling with different intensity, isothermal quenching) specimen were subjected to tempering in order to remove stresses (180 °C, 3 h).

Mechanical properties in uniaxial tension were determined in an Instron unit at room temperature according to GOST 1497 using standard cylindrical specimens (type III) with a gauge length diameter of 6 mm and gauge length 30 mm. Impact bending testing according to GOST 9454 was performed by means of a pendulum hammer with impact energy of 300 J. Standard specimens (type 11) were used with a V-shaped stress concentrator.

In order to reveal specimen microstructure they were subjected to grinding, polishing, and etching in 4% nitric acid solution in methanol. The microstructure was studied by an optical microscope (MEIJI IM7200) method at a magnification of X500–X1000.

X-ray structural phase analysis was carried within a Bruker D8 Advance X-ray diffractometer in K_α Co radiation in the range of reflection angles $2\theta = 45–140°$ with a voltage of U = 35 kV, tube current I = 40 mA. Quantitative X-ray phase analysis was conducted by the Reitveld standard-free complete profile analysis method using TOPAS 4.2 software.

Experimental results and discussion

Dilatometric study showed that during continuous cooling from the austenitizing temperature in the rate range 0.1–30 °C/sec within test steels no formation of a ferrite-pearlite mixture was observed. Martensitic transformation within the test steels during high-speed cooling of 30 °C/sec (Fig. 1a) commences at 360 °C (18Kh2N4MA), 335 °C (25KhN3MA), and 320 °C (25Kh2N4MA). A different temperature for the start of martensitic transformation is due to a different carbon content for the steel [22]: minimum (0.19 wt.%) for steel 18Kh2N4MA, maximum (0.27 wt.%) for steel 25Kh2N4MA.

With a reduction in cooling rate to 1 °C/sec within steels 18Kh2N4MA and 25Kh2N4MA the temperature for the start of supercooled austenite transformation is unchanged, although the course of the process differs somewhat (Fig. 1b and 2). In the case of cooling at a rate of 1 °C/sec up to the instant of achieving 70–80%

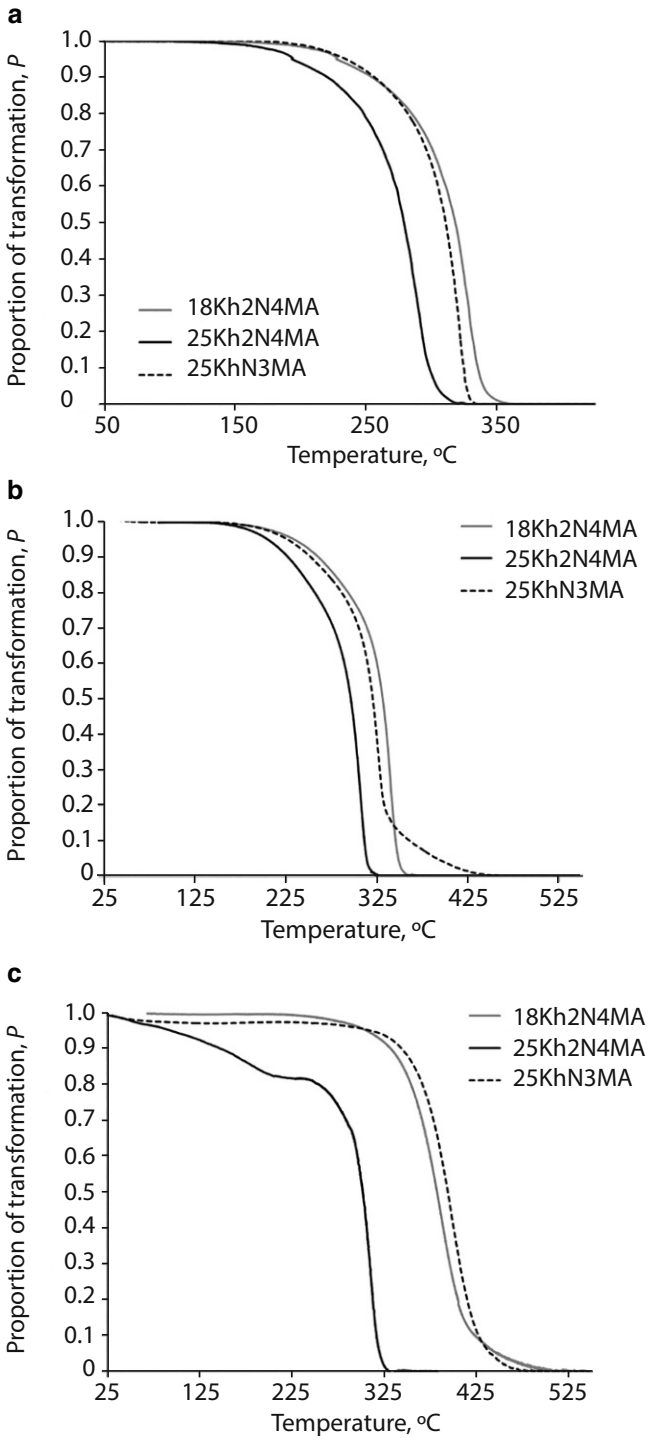

Fig. 1 Dependence of the proportion of austenite transformation on temperature during interrupted cooling for test steel s from 800 °C at rate: 30 °C/sec (**a**); 1 °C/sec (**b**); 0.1 °C/sec (**c**)

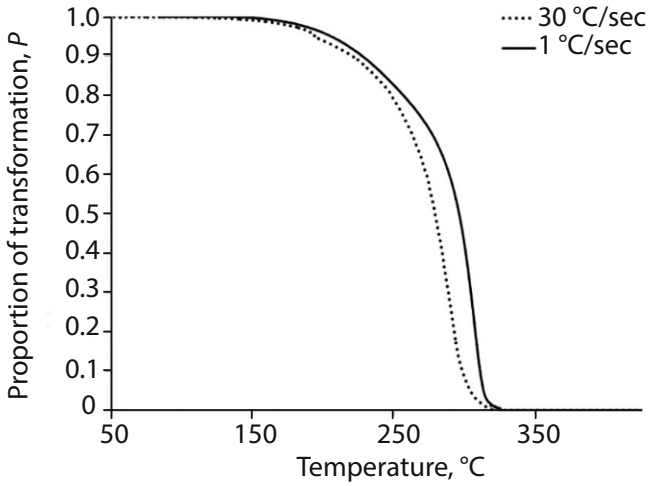

Fig. 2 Dependence of the proportion of austenite transformation on temperature during cooling for steel 25Kh2H4MA from 880 °C at rate of 1 and 30 °C/sec

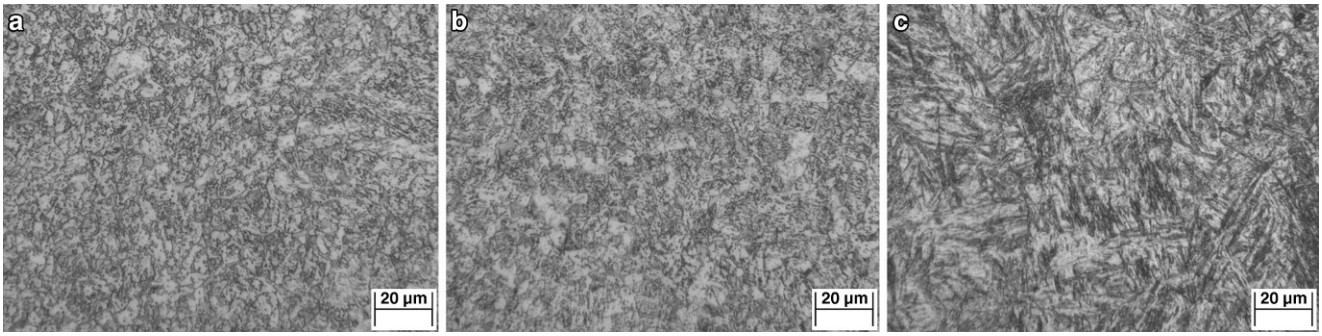

Fig. 3 Microstructure of test steels after cooling from 880 °C at rate of 0.1 °C/sec: 18Kh2N4MA (**a**); 25Kh2N3MA (**b**); 25KhN4MA (**c**)

of transformation more intense austenite decomposition is observed, after which the process develops in the same way as during cooling at a rate of 30 °C/sec. This is connected with the fact that with a little supercooling below the M_s temperature the transformation process is determined not only by temperature, which is typical for formation of athermal martensite, but also the cooling duration, that is the time. The latter is typical for bainitic transformation, which may be accomplished at a constant temperature during a determined time.

For steel 25KhN3MA a reduction in cooling rate from 30 to 1 °C/sec leads to a clear shift the temperature for the start of austenite breakdown in the region above M_s (see Fig. 1b). In this case the rate of bainite formation is quite slow, and starting from 445 °C towards the instant of reaching the M_s temperature (335 °C) there is formation of about 15% bainite. On reaching the M_s temperature significant acceleration of the process is observed, caused by simultaneous occurrence of martensitic and bainitic transformations.

With a further reduction in cooling rate within the steels studied there is formation of a greater amount of bainite, and the temperature for the start of supercooled austenite transformation increases (see Fig. 1c) to 500 °C (18Kh2N4MA), 480 °C (25KhN3MA), and 325 °C (25Kh2N4MA). It should be noted that for steel 25Kh2N4MA bainitic transformation in the cooling rate test range is implemented exclusively within the temperature range for martensitic transformation (below M_s). In this case cooling at a rate of 0.1 °C/sec bainite formation provokes diffusion redistribution of carbon between α-phase and untransformed austenite, which leads to enrichment of austenite with carbon and as a consequence to a reduction in the martensitic transformation temperature range. As a result at a temperature below 215–220 °C formation of martensite enriched with carbon commences. For steels 18Kh2N4MA and25KhN3MA this phenomenon is not observed, and with cooling at a rate of 0.1 °C/sec only bainite formation is recorded by dilatometry.

Therefore, within the steels studied bainite formation depending upon cooling rate in the range 0.1–30 °C/sec is partially or entirely implemented in the martensitic transformation temperature range.

A study of the microstructure showed that within steels 18Kh2N4MA and 25KhN3MA with slow cooling at a rate 0f 0.1 °C/sec there is formation predominantly of upper bainite, having a typical granular morphology (Fig. 3a, b) and hardness of 38–39 HRC. In steel 25Kh2N4MA bainite has a bundle structure (Fig. 3c) since there is formation within the martensitic transformation temperature region. The hardness of the bainitic-martensitic structure of steel 25Kh2N4MA after slow cooling comprises 47 HRC.

On the basis of these studies thermokinetic diagrams were plotted for supercooled austenite transformation of the steels studied (Fig. 4). As is seen, a reduction in carbon content from 0.19 wt.% (steel 18Kh2N4MA) (see Fig. 4a) to 0.27 wt.% leads to a shift in the bainitic transformation temperature range into a lower temperature region (below *M*s). For steel 25KhN3MA as a result of lower content of the main alloying elements compared with steel 25Kh2N4MA it exhibits a clearly deformed region of upper bainite formation (see Fig. 4b).

In order to evaluate the effect of temperature, with which there is bainite formation, on test steel structural composition dilatometric studies were performed for processes occurring during implementation of isothermal quenching. In the course of experiments transformation of supercooled austenite was recorded, proceeding

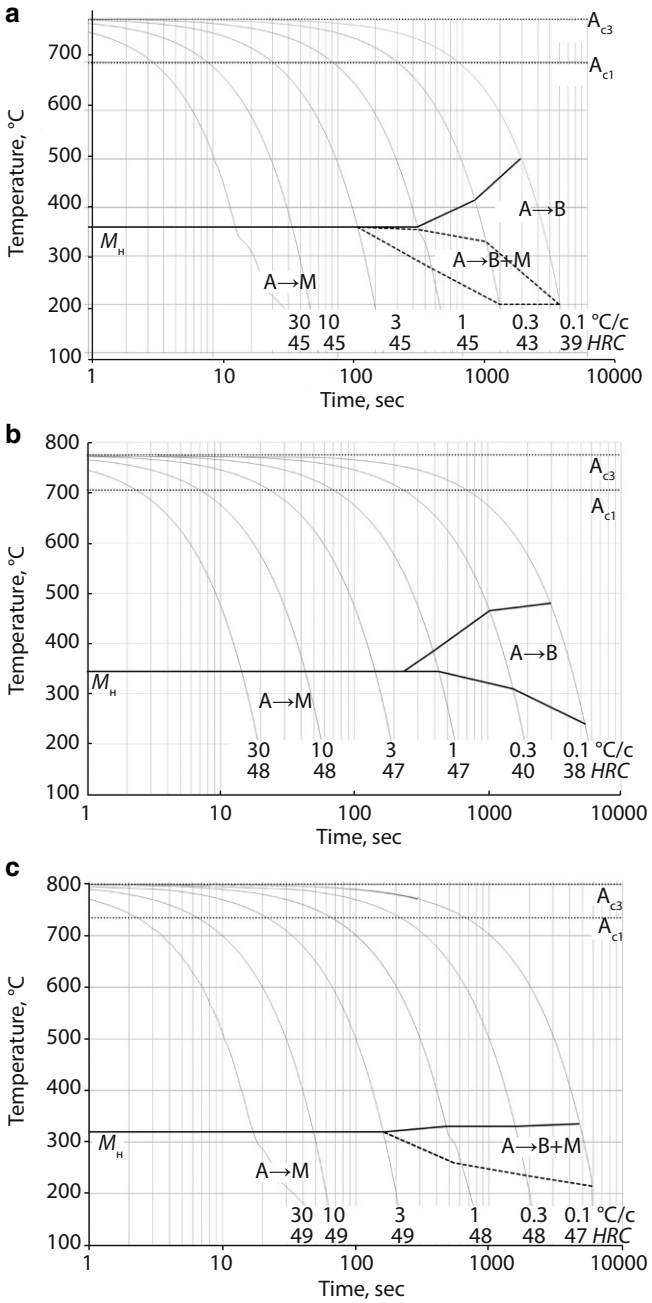

Fig. 4 Thermokinetic transformation diagrams for supercooled austenite within steels 18Kh2N4MA (**a**); 25Kh2N3MA (**b**); 25KhN4MA (**c**) (austenitizing temperature 880 °C)

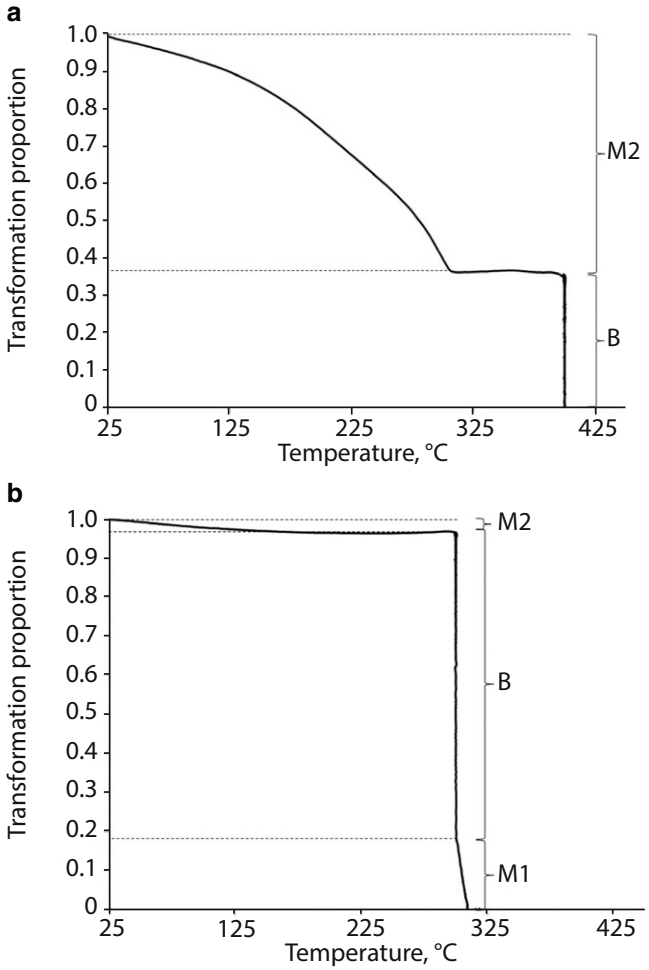

Fig. 5 Dependence of proportion of supercooled austenite transformation for steel 25Kh2n4MA on temperature during performance of dilatometric experiment using isothermal cooling: a isothermal exposure temperature 400 °C (above M_S); b isothermal exposure temperature 300 °C (below M_S)

during cooling from the austenitizing temperature to isothermal exposure, during exposure and after isothermal exposure with cooling to room temperature. As result of using Eq. 1 for analyzing experimental data curves were obtained for the dependence of the proportion of supercooled austenite transformation on temperature (Fig. 5), on which it is possible to observe temperature ranges for formation of some or other structural components during interrupted cooling before and after isothermal exposure, thereby an isothermal bainitic transformation on a curve is reflected in the form of a vertical line. For example, in the case of performing isothermal quenching for steel 18Kh2N4MA at a temperature above M_S transformation of supercooled austenite

commences with formation of bainite (B), and during subsequent cooling after isothermal exposure there is formation of "secondary" martensite (M2) enriched with carbon, having a reduced M_s temperature compared with the original steel composition (see Fig. 5a). in the case of performing isothermal quenching at a temperature below M_s on a curve formation of "primary" martensite (M1) is observed during cooling to the isothermal exposure temperature, formation of isothermal bainite (B) during exposure, and also formation of a small amount of "secondary" martensite (M2) during cooling to room temperature (Fig. 5b). In addition, the curves obtained make it possible to evaluate the quantitative ratio of structural components formed within the test steels after isothermal quenching at different temperatures (with the exception of residual austenite).

On the basis of the data obtained structural diagrams were plotted, reflecting the quantitative relationship of martensite and bainite within the test steels after isothermal quenching at different temperatures (Fig. 6). As is seen, the most extensive region for bainite within the structure of the diagram is typical for steel 25KhN3MA, exhibiting the least supercooled austenite stability. The maximum bainite content within the structure of each steel studied (about 80% for steel 18Kh2N4MA, 95% for steels 25KhN3MA and 25Kh2N4MA) is only achieved within the temperature in the M_s region. A marked reduction should be noted in the amount of "secondary" martensite (not more than 2–5%) within the test steel structure with a reduction in isothermal quenching temperature below the M_s. therefore, formation of "primary" martensite during cooling to the isothermal exposure temperature facilitates primarily more complete occurrence of bainitic transformation and secondly better stabilization of untransformed austenite during final cooling to room temperature.

Bainitic isothermal transformation kinetics within the test steels depend significantly upon the exposure temperature. It has been established (Fig. 7) that in the case of isothermal quenching at a temperature below M_s bainite formation commences rapidly at the instant of reaching the exposure temperature. With an increase in isothermal quenching temperature above the *M*s point the initial stage of bainite transformation slows down. This is connected with the fact that preliminary formation of "primary" martensite serves as a prepared substrate for the isothermal bainite formed. Stoppage of bainite transformation (emergence into a plateau) within steels 18Kh2N4MA and 25KhN3MA mainly occurs after 1000 and 1500 sec (for steel 25Kh2N4MA it is after 2500–3000 sec) after the start of isothermal exposure. However, with reduced process temperatures (250 °C) bainitic transformation continues for 3 h, and at the instant of completion of experimental exposure an equilibrium condition is not achieved.

Features of the isothermal bainitic transformation kinetics in the test steels at different exposure temperatures were analysed by means of the Austin-Rickett equation [23, 24]

$$P_b = 1 - \left[\frac{1}{1} + k\tau^n\right], \tag{2}$$

where P_b is the proportion of bainite; τ is time, sec; *k, n*, are coefficients constant in time, depending on the isothermal exposure temperature. By using an algorithm of successive iterations, implemented in a Microsft Excel medium, experimental dependences of the proportion of bainite on exposure time (see Fig. 7) approached to the maximum approximation by Eq. 2. In total temperature dependences were obtained for coefficients *n* and ln(*k*) for steels studied (Fig. 8). These dependences show a sharp change in the nature of bainitic transformation with an increase in exposure temperature above M_s. In the temperature range for martensitic transformation the value of coefficient *n* is 1.0–1.5, and in the case of isothermal transformation at a temperature above M_s the value of coefficient *n* increases to 2.0–2.5. The dependences obtained also have an extreme at 400 °C for steels 18Kh2N4MA and 25KhN3MA (see Fig. 8a, b) and at 330–370 °C for steel 25Kh2N4MA (see Fig. 8a).

Presence of an extremum on the temperature dependence for coefficients of Eq. 2 is connected with a change in morphology of the bainite formed [25]: preferentially upper bainite forms at a temperature above the extremum, and predominantly lower bainite forms at a temperature below the extremum. This is confirmed by metallographic study (Fig. 9). Lower bainite within the test steel, formed at a temperature below M_s, has a pack-

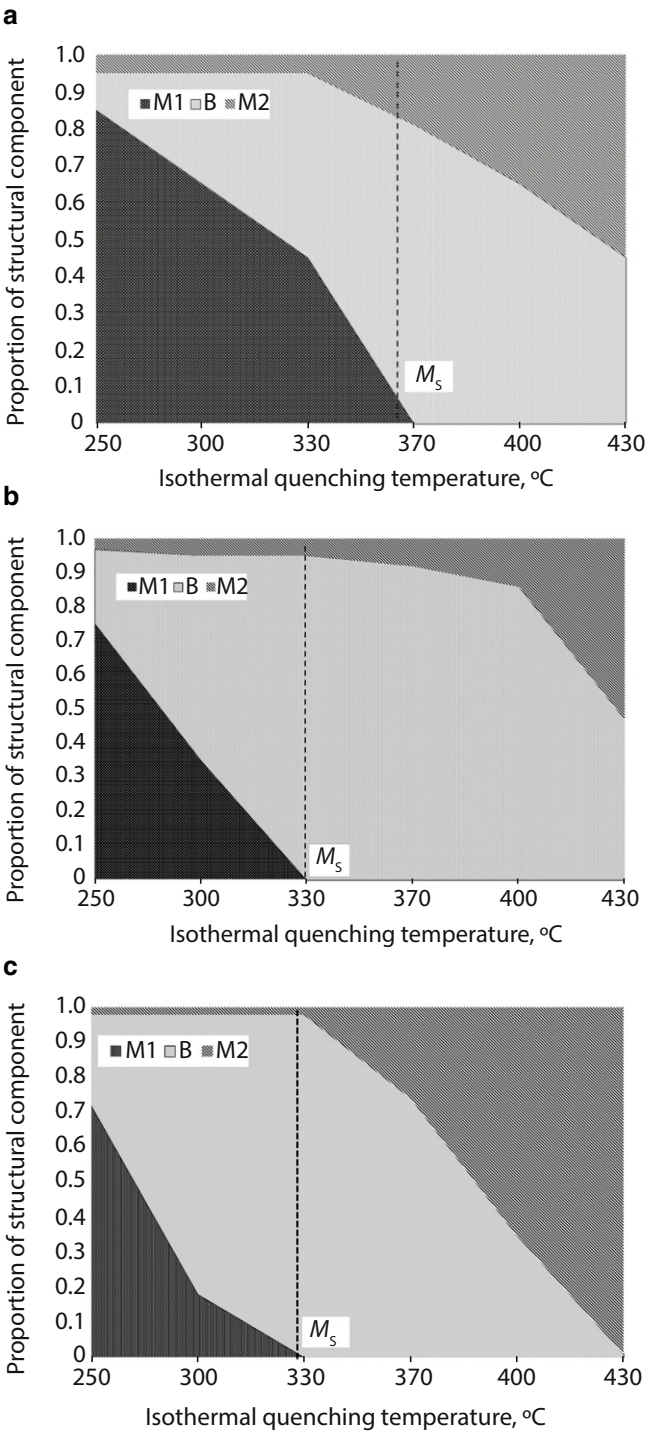

Fig. 6 Ratio of the amount of structural components formed within steel after isothermal quenching at different exposure temperatures: 18Kh2N4MA (**a**); 25Kh2N3MA (**b**); 25KhN4MA (**c**)

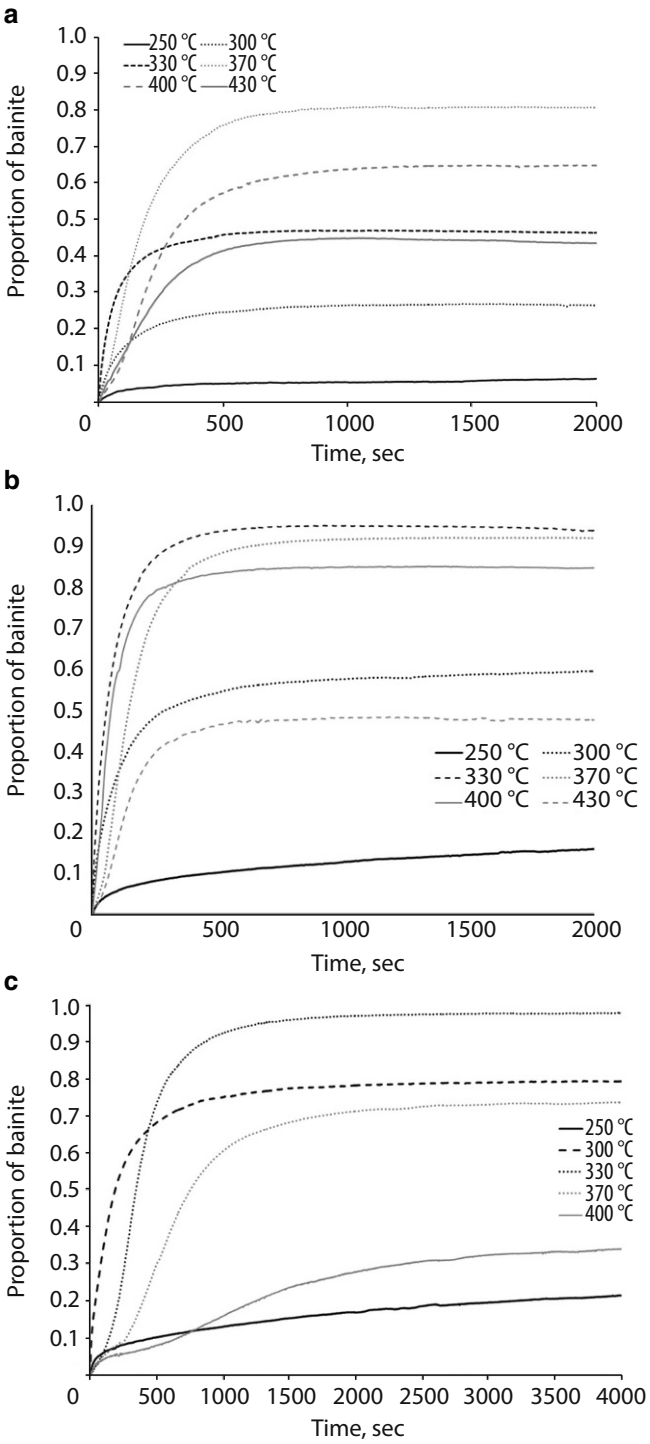

Fig. 7 Bainitic isothermal transformation kinetics at different exposure temperatures: 18Kh2N4MA (**a**); 25Kh2N3MA (**b**); 25KhN4MA (c)

https://doi.org/10.1007/s11015-024-01732-3

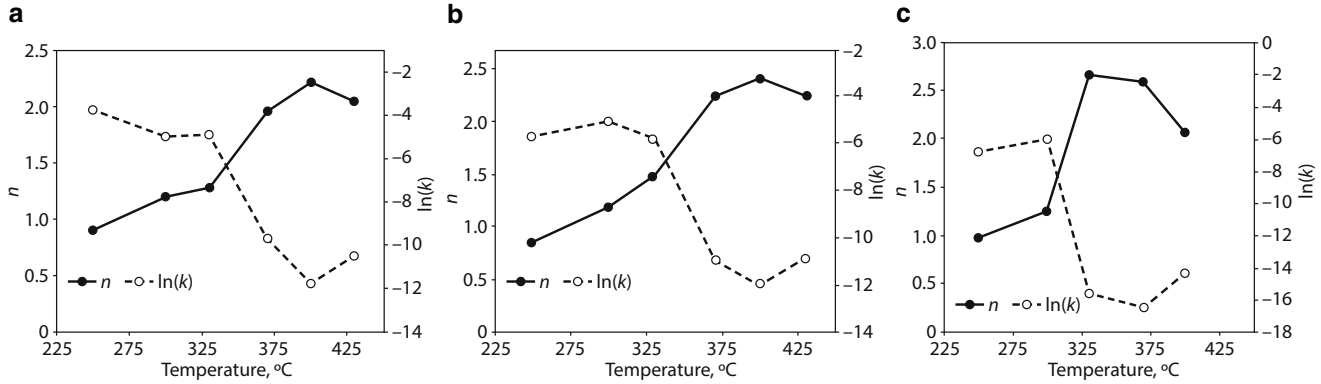

Fig. 8 Dependence of Austin-Rickett equation coefficients (2) on isothermal exposure temperature: 18Kh2N4MA (**a**); 25Kh2N3MA (**b**); 25KhN4MA (**c**)

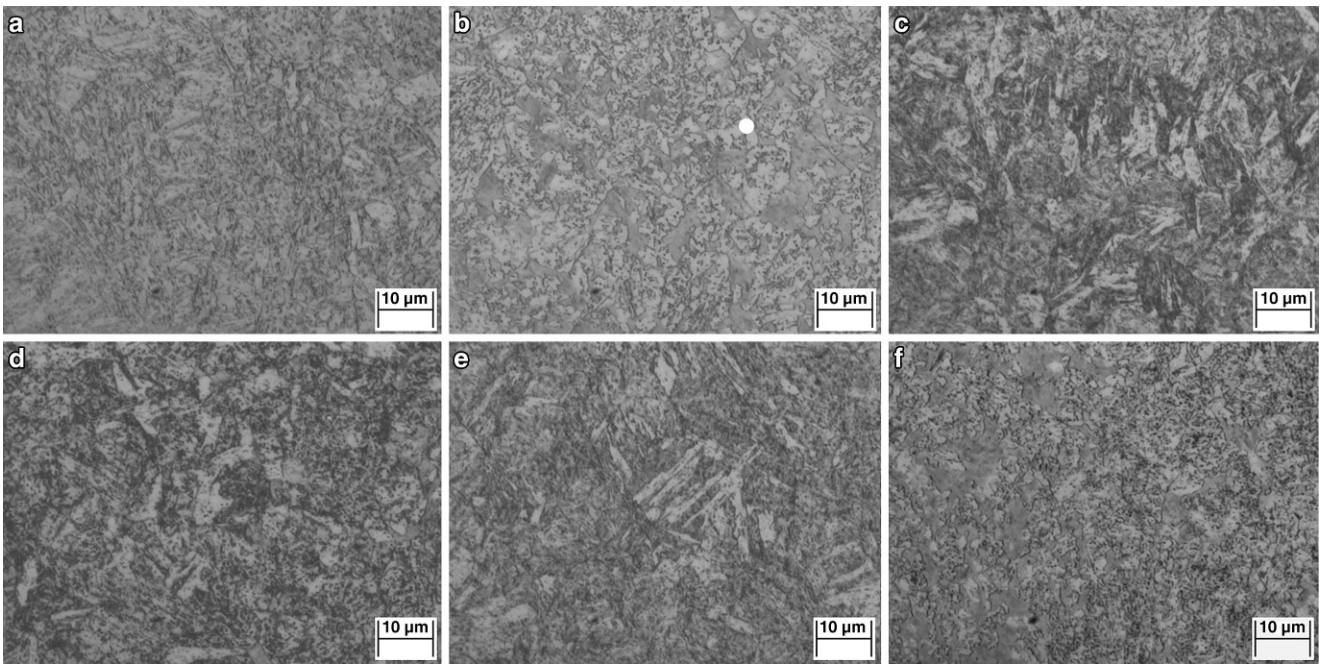

Fig. 9 Microstructure of steels 18Kh2N4MA (**a**, **b**); 25Kh2N3MA (**c**, **d**); 25KhN4MA (**e**, **f**) after isothermal quenching at temperature: 330 °C (**a**); 400 °C (**b**); 300 °C (**c**); 400 °C (**d**); 300 °C €; 370 °C (**f**)

age structure (see Fig. 9), i.e., it is formed in the shape of platelets, which is due to presence of previously formed bundles of martensite, which limits free space for growth of bainitic colony growth. This agrees with value of coefficient $n = 1.0–1.5$ obtained, which specify the spatial morphology of growing phase particles [8, 26], with an isothermal exposure temperature in the region of the extremum the upper bainite formed has granular morphology with visible precipitates of carbide particles (see Fig. 9b, d, f). In this case the value of coefficient $n = 2.0–2.5$ corresponds to conditions with which growth of bainitic colonies proceeds from grain boundaries or from interphase boundaries.

Within test steels during isothermal quenching it is almost impossible to obtain an entirely bainitic microstructure, and therefore in order to evaluate mechanical properties two temperatures were selected for isothermal exposure for each steel: from the region of formation of "primary" martensite and lower bainite formation (300–330 °C), from the region of upper bainite and "secondary" martensite formation (370–400 °C). Conditions

Table 2 Microstructure Composition and Mechanical Properties of Test Steels after Isothermal quenching*

Steel	*t*, °C	P_B	P_A	P_A	$\sigma_{0.2}$, MPa	Σ_w, MPa	δ, %	ψ, %	*KC*V, MJ/m^2	*KC*V/KCV(M)
Upper bainite + *M2*										
18Kh2N4MA	400	0.58	0.31	0.11	1100	1325	12.0	57.9	0.8	0.75
25Kh2N3MA	400	0.77	0.14	0.09	90	1260	12.5	49.7	0.4	0.68
25KhN4MA	370	0.65	0.21	0.14	1050	1375	12.0	43.8	0.5	0.98
Lower bainite + M1 (P_{M2} = 0.02–0.05)										
18Kh2N4MA	330	0.47	0.42	0.06	950	1220	14.0	61.3	1.3	1.24
25Kh2N3MA	300	0.58	0.34	0.04	1255	1465	12.5	62.9	0.6	1.00
25KhN4MA	300	0.78	0.17	0.03	1200	1440	13.0	58.7	0.6	1.25

**Note*: P_B is proportion of bainite, P_M is proportion of martensite ("primary" or "secondary"), *P*A is proportion of residual austenite, *KCV*/*KCV*(M) is ratio of mixed structure impact strength, containing bainite, to impact strength of entirely martensitic structure (Table 3)

Table 3 Test Steel mechanical Properties after Cooling from Austenitizing Temperature 880 °C within Different Media

Steel	Cooling medium	$\sigma_{0.2}$, MPa	Σ_w, MPa	δ, %	ψ, %	*KC*V, MJ/m^2	P_A
18Kh2N4MA	Oil	1234	1423	12.9	62.3	1.0	0.04
	Air	1097	1381	14.3	63.8	1.1	0.05
	Container	983	1214	14.5	62.1	1.4	0.10
25Kh2N3MA	Oil	1361	1588	12.8	60.1	0.6	0.05
	Air	1192	1440	13.1	60.0	0.7	0.06
	Container	961	1246	13.6	51.0	0.4	0.09
25KhN4MA	Oil	1403	1632	11.7	55.3	0.5	0.04
	Air	1342	1648	10.7	48.7	0.4	0.06
	Container	1306	1520	11.1	52.8	0.5	0.10

for conducting heat treatment, quantitative composition of the microstructure based upon dilatometric and X-ray structural analysis data, and the corresponding mechanical properties for the steels are provided in Table 2.

The results obtained show that the test steel microstructure containing upper bainite exhibits reduced impact strength both compared with a mixture of upper bainite and "primary" martensite, and also compared with an entirely martensitic structure after oil quenching (Table 3): the ratio of the impact strength of a structure containing upper bainite to impact strength of a martensitic structure KCV/KCV(M) < 1. In this case formation of lower bainite within steels 18Kh2N4MA and 25Kh2N4MA leads to an increase in impact strength by 25% with respect to an entirely martensitic structure in spite of the fact that after isothermal quenching in the lower bainite temperature range the amount of residua austenite stabilized within the test steels comprises in total 3–6%, which is 2–4 times less than after isothermal quenching in the temperature range for formation of upper bainite (9–14%). A higher residual austenite content within a mixed structure of upper bainite and "secondary" martensite also cannot lead to the expected increase in steel ductility. This is connected: (1) with formation of carbide during upper bainite formation [11], which coarsens the interphase boundaries between α- and γ-phases; (2) with formation during final cooling of "secondary" martensite enriched with carbon, whose ductility is lower than for low-carbon martensite (within the scope of the present study it has been demonstrated that even an increase in carbon content from 0.19 wt.% in steel 18Kh2N4MA to 0.27 wt.% in steel 25Kh2N4MA leads to a reduction in martensite impact strength by a factor of two, see Table 3).

It should be noted that isotheral quenching of steel 25KhN3MA in the temperature range for lower bainite formation does it make it possible to obtain a better impact strength compared with entirely martensitic structure. This is connected with the fact that cooling to an isothermal exposure temperature in specimens of this steel manages to form some amount of upper bainite as a result of lower supercooled austenite stability.

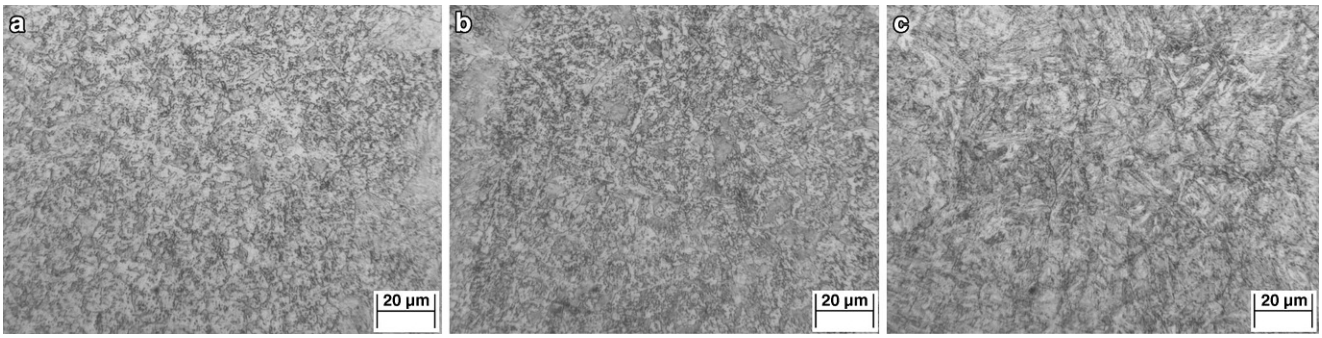

Fig. 10 Test steel microstructure after cooling from 880 °C within heat insulated container (average cooling rate 0.2 °C/sec)

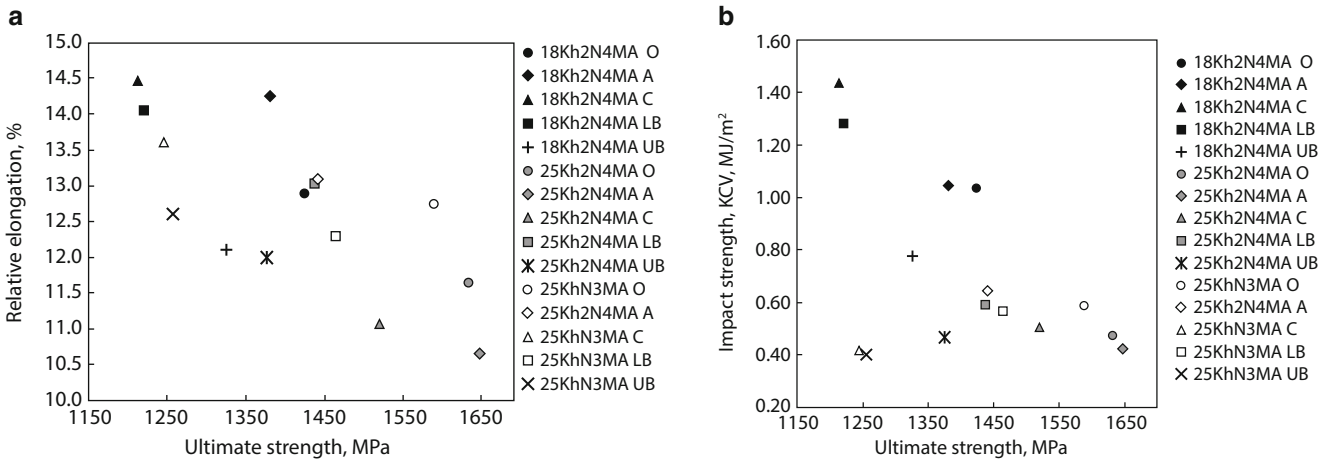

Fig. 11 Diagrams of mechanical properties obtained as a result of test steel heat treatment: **a** strength—ductility; **b** strength—impact strength (*O* is cooling in oil; *A* is cooling within still air; is cooling within heat-insulated chamber; *LB* is isothermal quenching in lower bainite region; *UB* is isothermal quenching within upper bainite region)

From Table 3 it is seen that a reduction in quenching cooling intensity from 25 °C/sec (cooling in oil) to 0.2 °C/sec (cooling within a container) for the test steels containing carbon more than 0.25 wt.% leads either to a reduction in impact strength (25KhN3MA), or it has almost no effect on this value (25Kh2N4MA) this is determined by the amount of upper bainite formed within steel during cooling. Steel 25KhN3MA has a broader temperature range for bainite formation compared with steel 25Kh2N4MA (see Fig. 4 and 6), and as a result of slow cooling within it there is formation of a significant amount of upper bainite, and reduced steel toughness-ductility properties (Fig. 10).

In spite of the fact that within steel 18Kh2N4MA with slow cooling within a heat-insulated container there is also formation of upper bainite (see Fig. 10a), nonetheless the level of impact strength (1.4 MJ/m^2) is considerably higher than after oil quenching (1.0.mJ/m^2), and after isothermal quenching in the upper bainite temperature range (0.8 mJ/m^2). This is due to formation within steel 18Kh2N4MA of a complex microstructure containing smaller amount of martensite enriched with carbon. In addition, in steel 18Kh2N4MA there is the least carbon content within the steels studied, and therefore even upper bainite within this steel exhibits better impact strength than lower bainite within steels 25Kh2N4MA and 25KhN3MA (see Table 2).

It should be noted that a reduction in cooling intensity for all of the test steels leads to an increase in the residual austenite content from 4–5% to 9–10%, which causes an increase in relative elongation with presence of α-bainite after cooling steels 18Kh2N4MA and25Kh2N4MA. Steel 25Kh2N4MA with the greatest supercooled austenite stability, and not inclined towards formation of a significant of upper bainite even with slow cooling within a container, provides a stable set of toughness-ductility properties over a wide range of cooling intensity

(from 25 to 0.2 °C/sec). In this case the strength of steel 25Kh2N4MA is also reduced to a lesser extent (by 7%) with a reduction in quenching cooling rate compared with steel 18Kh2N4MA (reduction in strength by 15–20%) and 25KhN3MA (reduction in strength by 20–30%).

Comparative mechanical properties are provided in Fig. 11, achieved after different hat treatment regimes for the test steels. In a diagram on coordinates "strength—ductility" (see Fig. 11a) a well-known tendency is observed towards an increase in ductility with a reduction in strength [27]. According to this diagram steel 18Kh2N4MA after cooling within still air, within a heat-insulated container, and after isothermal quenching for lower bainite, may conditionally be referred to high-strength steels of a third generation, used within automobile building [28, 29]. In this case the good austenite stability for steel 18Kh2N4MA makes it possible to simplify component heat treatment technology, since in this case it is unnecessary to conduct rapid cooling in order to achieve formation of a ferrite-pearlite mixture.

With use of a diagram on strength-ductility coordinates (see Fig. 11b) a tendency is also observed towards an increase in steel impact strength with a reduction in strength. However, in the case of steel 25KhN3MA after slow cooling within a container and after isothermal quenching at 400 °C (in all cases within the steel structure there is formation of upper bainite) there is a reduction simultaneously in both strength and impact toughness. It should be noted that in this case at the same level of strength (1200–1250 MPa) within steel 18Kh2N4MA reaches impact strength of 1.3–1.4 MJ/m^2.

Therefore, upper bainite formation within steels affects in a differ way impact strength indices: within steel 18Kh2N4MA presence of upper bainite alongside lower bainite leads to an increase in impact strength; within steel 25KhN3MA it leads to a reduction. This is due to the carbon content within steel, and as a consequence processes of carbide formation during bainitic transformation. The bainite transformation characteristics obtained within chromium-nickel-molybdenum carburized steels should be considered in developing chemical heat treatment technology for components.

Conclusions

1. Thermokinetic diagrams have been plotted for transformation of supercooled austenite within steels 18Kh2N4MA, 25Kh2N4MA, 25KhN3MA with uninterrupted cooling to the austenitizing temperature 880 °C at a constant rate of 0.1–30 °C/sec. It is shown that within the test steels studied bainite formation in relation to cooling rate is partly or entirely realized within the temperature range for martensitic transformation (below the M_s temperature).
2. During isothermal quenching in the temperature region above *M*s within test steel structure there is formation of bainite with a significant amount of "secondary" martensite, having a reduced M_s temperature compared with the original steel composition. In the case of isothermal quenching at a temperature below the M_s within the steel structure there is formation within the steel structure of "primary" martensite, bainite, and a small amount of (< 5%) "secondary" martensite.
3. It has been shown that the temperature range for martensitic transformation of bainite forms in the form of platelets or needles, which is due to presence of previously formed bundles of martensite, and in the case of isothermal transformation at a temperature above Ms the growth of bainitic colonies proceeds from grains boundaries or from interphase boundaries. It has been established that the quantitative ratio of structural components forms as a results of isothermal quenching at different temperatures. It has been shown that the greatest amount of bainite within the structure of each of the test steels (about 80% for steel 18Kh2N4MA, more than 95% for steels 25KhN3MA and 25Kh2N4MA) is only achieved with an isothermal quenching temperature within the M_s region.
4. Formation of upper bainite within steels ambiguously affects impact strength indices: within steel 18Kh2N4MA a mixture of upper and lower bainite after slow cooling provides an impact strength of 1.4 MJ/m^2; within steel

25KhN3MA it is 0.4 MJ/m^2. Steel 25Kh2N4MA exhibits stable strength properties (1400–1650 MPa), ductility (11–13%), and impacts strength (0.4–06 MJ/m^2) with implementation of different versions of strengthening heat treatment.

5. Within steel 18Kh2N4MA after cooling at a rate of 1.0 and 0.2 °C/sec and after isothermal quenching for lower bainite simultaneously high strength (1200–1250 MPa), ductility (14–15%) and impact strength (1.3–1.4 MJ/m^2) are achieved, and it is possible to relate it to high-strength steels of a third generation for automobile building.

Funding Research conducted due to a grant from the Russian scientific fund No. 22-29-00106.

References

1. Song W, Lei M, Wan M, Huang C (2021) Continuous cooling transformation behaviour and bainite transformation kinetics of 23CrNi3Mo carburised steel. Metals 11(1):48. https://doi.org/10.3390/met11010048
2. Torsten H, Olsson P, Troell E (eds) (2012) Steel and its heat treatment. A handbook. Swerea IVF, Sweden
3. Maisuradze MV, Yudin YV, Kuklina AA (2019) Increase in impact strength during bainite structure formation in HY-TUF high-strength steel. Metallurgist 63(7/8):849–858. https://doi.org/10.1007/s11015-019-00899-4
4. Yu. Kaletinm A, Ryzhkov AG, Kaletina YV (2015) Increase in structural steel impact strength with formation of carbide-free bainite. FMM 116(1):114–120
5. Suh M-S, Nahm S-H, Suh C-M, Park N-K (2022) Impact toughness of spring steel after bainite and martensite transformation. Metals 12(2):304. https://doi.org/10.3390/met12020304
6. Caballero FG, Roelofs H, Hasler S, Capdevila C, Chao J, Cornide J, Garcia-Mateo C (2012) Influence of bainite morphology on impact toughness of continuously cooled cementite free bainitic steels. Mater Sci Techn 28(1):95–102. https://doi.org/10.1179/1743284710Y.0000000047
7. Maisuradze MV, Kuklina AA, Lebedev DI, Nazarova VV, Antakov EV, Yurovskikh AS (2023) Simulated and experimental study of structure formation upon thermal treatment of steel 20Kh2G2SNMA. Steel Transl 53(2):176–184. https://doi.org/10.3103/S0967091223020122
8. Zhu JG, Sun X, Barber GC, Han X, Qin H (2020) Bainite transformation-kinetics-microstructure characterization of austempered 4140 steel. Metals 10(2):236. https://doi.org/10.3390/met10020236
9. Bakhtiari R, Ekrami A (2009) The effect of bainite morphology on the mechanical properties of a high bainite dual phase (HBDP) steel. Mater Sci Eng A 525(1–2):159–165. https://doi.org/10.1016/j.msea.2009.07.042
10. Hajizad O, Kumar A, Li Z, Petrov RH, Sietsma J, Dollevoet R (2019) Influence of microstructure on mechanical properties of bainitic steels in railway applications. Metals 9(7):778. https://doi.org/10.3390/met9070778
11. Bhadeshia HKDH, Honeycombe R (2017) Steels: microstructure and properties. Elsevier, Oxford
12. Lawrynowicz Z (2002) Carbon partitioning during bainite transformation in low alloy steels. Mater Sci Techn 18(11):1322–1324. https://doi.org/10.1179/026708302225007259
13. Clarke AJ, Speer JG, Miller MK, Hackenberg RE, Edmonds DV, Matlock DK, Rizzo FC, Clarke KD, De Moor E (2008) Carbon partitioning to austenite from martensite or bainite during the quench and partition (Q&P) process: a critical assessment. Acta Mater 56(1):16–22. https://doi.org/10.1016/j.actamat.2007.08.051
14. Lin S, Borgenstam A, Stark A, Hedström P (2022) Effect of Si on bainitic transformation kinetics in steels explained by carbon partitioning, carbide formation, dislocation densities, and thermodynamic conditions. Mater Charact 185:111774. https://doi.org/10.1016/j.matchar.2022.111774
15. He B (2020) On the factors governing austenite stability: intrinsic versus extrinsic. Materials 13(15):3440. https://doi.org/10.3390/ma13153440
16. Abbaszadeh K, Saghafian H, Kheirandish S (2012) Effect of bainite morphology on mechanical properties of the mixed bainite-martensite microstructure in D6AC steel. J Mater Sci Techn 28(4):336–342. https://doi.org/10.1016/S1005-0302(12)60065-6
17. Yao Z, Li M, Hu H, Tian J, Xu G (2021) Microstructure and wear properties of a bainite/martensite multi-phase wear resistant steel. ISIJ Intern 61(1):434–441. https://doi.org/10.2355/isijinternational.ISIJINT-2020-327
18. Maisuradze MV, Yudin YV, Kuklina AA, Lebedev DI (2023) Effect of heat treatment on mechanical properties and microstructure of advanced high-strength steel. Met Sci Heat Treat 64(9/10):565–571. https://doi.org/10.1007/s11041-023-00845-x
19. Kop TA, Sietsma J, Van Der Zwaag S (2001) Dilatometric analysis of phase transformations in hypo-eutectoid steels. J Mater Sci 36:519–526. https://doi.org/10.1023/A:1004805402404
20. Ryzhkov MA, Popov AA (2011) Methodological aspects of plotting of thermokinetic diagrams of transformation of supercooled austenite in low-alloy steels. Met Sci Heat Treat 52:612–616. https://doi.org/10.1007/s11041-011-9329-7

21. Maisuradze MV, Kuklina AA, Ryzhkov MA, Lebedev DI, Antakov EV (2022) Effect of cooling rate during heat treatment on martensitic-bainitic class alloy steel micro-structure and properties. Metallurgist 66(7/8):895–908. https://doi.org/10.1007/s11015-022-01402-2
22. Maisuradze MV, Ryzhkov MA, Antakov EV, Popov NA, Proskuryakov PA (2020) Special features of transformations of supercooled austenite in modern structural steels. Met Sci Heat Treat 62(7/8):448–456. https://doi.org/10.1007/s11041-020-00583-4
23. Austin JB, Rickett RL (1939) Kinetics of the decomposition of austenite at constant temperature. Trans Am Inst Min Metall Eng 964:1–20
24. Starink MJ (1997) Kinetic equations for diffusion-controlled precipitation reactions. J Mater Sci 32:4061–4070. https://doi.org/10.1023/A:1018649823542
25. Maisuradze MV, Yudin YV, Kuklina AA (2019) A novel approach for analytical description of the isothermal bainite transformation in alloyed steels. Mater Perform Charact 8(2):80–95. https://doi.org/10.1520/MPC20170168
26. Christian JW (2002) The theory of transformations in metals and alloys. Pergamon, Amsterdam
27. Santos RO, Moreira LP, Butuc MC, Vincze G, Pereira AB (2022) Damage analysis of third-generation advanced high-strength steel based on the Gurson–Tvergaard–Needleman (GTN) model. Metals 12(2):214. https://doi.org/10.3390/met12020214
28. Tisza M (2021) Three generations of advanced high strength steels in the automotive industry. In: Vehicle and Automotive Engineering 3. VAE 2020. Lecture notes in mechanical engineering. Springer, Singapore https://doi.org/10.1007/978-981-15-9529-5_7
29. Bleck W, Brühl F, Ma Y, Sasse C (2019) Materials and processes for the third generation advanced high-strength steels. Berg Huettenmaenn Monatsh 164:466–474. https://doi.org/10.1007/s00501-019-00904-y

Authors and Affiliations

M. V. Maisuradze[1] · A. A. Kuklina[1,2] · V. V. Nazarova[1] · M. A. Ryzhkov[1] · E. V. Antakov[1]

✉ M. V. Maisuradze
m.v.maisuradze@urfu.ru

[1] B. N. Yeltsin Ural Federal University, Yekaterinburg, Russian Federation

[2] Ural State Mining University, Yekaterinburg, Russian Federation